

Received 7 August 2023, accepted 13 September 2023, date of publication 20 September 2023, date of current version 2 October 2023.

Digital Object Identifier 10.1109/ACCESS.2023.3317514



Tunable Predefined Time Nonsingular Terminal Sliding Mode Control Based on Neural Network for Nonlinear Systems

CHAO JIA[®] AND XIAOHUA LIU

School of Electrical Engineering and Automation, Tianjin University of Technology, Tianjin 300384, China

Corresponding author: Chao Jia (jacky20042004@126.com)

This work was supported in part by the National Natural Science Foundation of China under Grant 62103298, in part by the Natural Science Foundation of Tianjin under Grant 18JCYBJC87700, and in part by the Training Plan for Young and Middle-Aged Backbone Innovative Talents in Colleges and Universities in Tianjin.

ABSTRACT This paper proposes a novel predefined time nonsingular terminal sliding mode control (TSMC) based on radial basis function neural network (RBFNN) for nonlinear systems. Firstly, a new lemma of tunable predefined time stability (PTS) is proposed, where the introduction of an adjustable parameter can adjust the stability time of the system and makes the design of the controller more flexible. Secondly, based on the proposed lemma, a new control method is proposed, which not only guarantees the PTS of the system, but also solves the singularity problem of the traditional TSMC and the problem of unknown model information. Finally, through comparative simulation, it is verified that the proposed method has good control performance.

INDEX TERMS Terminal sliding mode control, predefined time control, neural network control, robust nonlinear control, nonsingular control.

I. INTRODUCTION

In this era of rapid development of science and technology, people need to keep improving the performance of actual industrial systems. Any actual physical system is more or less nonlinear, such as hydraulic servo system [1], robot control system [2], multi-agent [3], spacecraft system [4] and so on. Control methods for nonlinear systems have sprung up rapidly, such as backstepping control [5], [6], sliding mode control (SMC) [4], [7], [8], adaptive control [9], etc. Among them, SMC has been widely studied by scholars due to its strong robustness and ability to handle disturbances [10], [11].

However, SMC can only ensure asymptotic stability, and its convergence time cannot be estimated, which seriously affects control efficiency. Tasks such as emergency rescue, missile launch, and rocket launch need to be completed within the specified time, otherwise significant losses will be caused,

The associate editor coordinating the review of this manuscript and approving it for publication was Vivek Kumar Sehgal.

which limits the application of SMC. Therefore, while ensuring that the system achieves the expected control objectives, it is also necessary to ensure that the convergence time (CT) is within the predefined range as much as possible. In order to meet the above requirements, Bhat et al. [12] proposed the concept of finite time control. Compared with asymptotic stability, it improves the convergence speed of the system states and enables them to converge within a finite time. Reference [13] added a linear term to sliding surface to enable the system states to converge at a faster rate and provided an expression for the CT. However, the CT of finite time control algorithms depends on the initial states of the system. If the initial values of the system are not appropriate, it will seriously affect the stability. Fortunately, Polyakov et al. [14] proposed a fixed time control method, ensuring that the upper bound of the CT is a constant. However, the relationship between control parameters and CT is often complex, and the estimation of CT is too conservative. To further solve this problem, a predefined time control algorithm was proposed, which can predetermine the convergence time boundary [15]. Due to this



major advantage, predefined time control algorithms have been applied in practical systems such as aerospace [16] and underwater robots [17]. Reference [18] proposed a predefined time SMC algorithm to ensure that the arrival phase in SMC is predefined time stable. Reference [19] designed a predefined time attitude tracking controller for the attitude tracking problem of rigid spacecraft. Reference [20] proposed a predefined time attitude stability control scheme for aircraft attitude stability.

Based on the above literature and reading other relevant literature, we find that the following difficulties still need to be addressed: (1) The controllers designed in References [19] and [20] have negative exponential terms, which can lead to the singular problem. If this problem is not solved, in some cases the amplitude of the controller will be very large, which does not match the actual situation. Therefore, this paper addresses the singular problem while ensuring PTS of the system. (2) Most of the existing literature on predefined time stability (PTS) has not considered the issue of unknown model information. Although RBFNN is unilized to approximate terms with unknown model information in [21], [22], and [23], only finite time or fixed time stability can be ensured, which upper bound of CT is influenced by the initial states or controller parameters. This paper will further research how to achieve PTS using RBFNN, while keeping the upper bound of CT set by the user themselves. (3) When the system stabilizes within the predefined time range, the actual CT is not adjustable. For example, if the user sets a predefined time of 8 s, the actual CT of the system needs to meet T < 8s, and the actual CT may be 1 s, 4 s or 7 s. How to design an algorithm to adjust the actual CT and make the predefined time closer to the user requirement is a major challenge.

Based on the above analysis and discussion, this paper proposes a novel predefined time nonsingular TSMC based on RBFNN. The main contributions are as follows:

- (1) Based on the tunable PTS definition, this paper proposes a new tunable PTS lemma. Compared with Lemma 1, the proposed lemma introduces adjustable parameters, making the design of the controller more flexible and can adjust the actual CT of the system.
- (2) Based on the proposed lemma, this paper designs a new control method to ensure that the system can achieve PTS during both sliding and arrival stages.
- (3) Inspired by the Reference [24], this paper proposes a new method by introducting a saturation function (SF). Thus we not only solve the singular problems, but also guarantee the predefined time stability of the system, which is not considered in Reference [24].
- (4) In this paper, a new controller based on RBFNN is designed, which not only solves the problem of unknown model information, but also ensures that the system converges to the sliding surface in a predefined time. A complet proof of PTS based on Lyapunov method is presented here.

II. PREPARATION AND PROBLEM FORMULATION

A. KEY DEFINITIONS AND LEMMAS

Consider a nonlinear system:

$$\dot{x} = f(x, t) \quad x(0) = x_0$$
 (1)

where $x \in \mathbb{R}^n$ represents the system states. Function: $f: \mathbb{R}^n \to \mathbb{R}^n$ is nonlinear and continuous, and f(0) = 0.

Lemma 1 [15]: For the system (1), if there is a Lyapunov function V(x), it satisfies the following conditions

$$\dot{V} \le -\frac{\pi}{\alpha T_c} (V^{1-\frac{\alpha}{2}} + V^{1+\frac{\alpha}{2}}) \tag{2}$$

Then the system (1) is predefined time stable. $T_c > 0$ is the predefined time, $0 < \alpha < 1$.

Definition 1 [15]: If the equilibrium point of the system (1) is stable in a finite-time, and $T: R^n \to R$ satisfies: $T(x_0, \mu) \le T_c$, $\forall x_0 \in R^n$, then the equilibrium point of the system (1) is considered to be tunable predefined-time stable, T_c is a predefined time. μ represents a tunable parameter.

Remark 1: Compared with fixed time control, the upper bound of the convergence time of the proposed method in this paper is set by the user, which is independent of the controller parameters. Compared with traditional PTS, the advantage of tunable PTS not only ensures the predefined time stability, but also enables the actual CT of the system to be adjustable.

Lemma 2: If there exists a positive definite function V(x) for the system (1) defined on the set U, for any $x \in U_0 \setminus \{0\}$, the set $U_0 \subseteq U$, V(x) satisfies the following formula

$$\dot{V} \le -\frac{\pi}{\alpha \mu T_c} (V^{1 - \frac{\alpha}{2}} + \mu^2 V^{1 + \frac{\alpha}{2}}) \tag{3}$$

where $0 < \alpha < 1, T_c > 0, \mu > 0$.

Then the system (1) is tunable predefined-time stable. T_c is the predefined-time.

Proof 1: According to Eq. (3), we can obtain

$$-\frac{\pi}{\alpha\mu T_c}dt \ge \frac{dV}{V^{1-\frac{\alpha}{2}} + \mu^2 V^{1+\frac{\alpha}{2}}} \tag{4}$$

Assuming T^* is the stable time of system (1), i.e. $V(T^*) = 0$ and $V(0) = v_0 > 0$.

Integrating from 0 to T^* , one gets

$$-\frac{\pi}{\alpha \mu T_c} \int_0^{T^*} dt \ge \int_{V(0)}^{V(T^*)} \frac{dV}{V^{1-\frac{\alpha}{2}} + \mu^2 V^{1+\frac{\alpha}{2}}}$$
 (5)

Then

$$\frac{\pi}{\alpha \mu T_c} \int_0^{T^*} dt \le \int_0^{\nu_0} \frac{dV}{V^{1 - \frac{\alpha}{2}} + \mu^2 V^{1 + \frac{\alpha}{2}}} \\
\le \int_0^{\nu_0} \frac{V^{\frac{\alpha}{2} - 1} dV}{1 + \mu^2 V^{\alpha}} \\
\le \frac{2}{\alpha \mu} \int_0^{\nu_0} \frac{d\mu V^{\frac{\alpha}{2}}}{1 + \mu^2 V^{\alpha}} \tag{6}$$

Then

$$\frac{\pi}{\alpha \mu T_c} T^* \le \frac{2}{\alpha \mu} \arctan(\mu v_0^{\frac{\alpha}{2}}) \tag{7}$$



According to the properties of the function $\arctan(x)$, its maximum value is $\frac{\pi}{2}$, we can obtain

$$T^* \le T_c \frac{2}{\pi} \arctan(\mu v_0^{\frac{\alpha}{2}}) \le T_c \tag{8}$$

Then the system (1) is tunable predefined time stable. T_c is the predefined time. This ends the proof.

Remark 2: Compared with Lemma 1, the proposed Lemma 2 introduces an adjustable parameter μ , which not only ensures predefined time stability, but also can adjust the actual CT by adjusting the value of μ . When $\mu=1$, Lemma 1 is a special case of Lemma 2. According to Eq. (2), in spite of the control gain α exists, the upper bound T_c of the CT is set by the user in advance and cannot be changed. Here the major role of α is to stabilize the system. According to the property of the predefined time stability, the value range of α is limited and the adjustable range is very small. Therefore, the adjustable parameter μ introduced in this article. It makes the actual CT of the system can be adjusted by adjusting parameter μ , which conforms to the Definition 1.

Remark 3: In actual control engineering, we expect to know the time of system stability. For the finite time control and fixed time control, we can obtain the upper bound of the convergence time, but the upper bound values obtained by the above methods are either related to the system states or to the controller parameters. The advantage of predefined time control is that the upper bound of the convergence time is set by the user and is independent of the system states and controller parameters. For example, if we require the task to be completed within 8 s, we need to set the parameter T_c to 8s in the predefined time algorithm, which is set by the user according to the actual needs.

Lemma 3: If there exists a positive definite function V(x) for the system (1) defined on the set U, for any $x \in U_0 \setminus \{0\}$, the set $U_0 \subseteq U$, V(x) satisfies the following formula

$$\dot{V} \le -\frac{\pi}{\alpha \mu T_c} (V^{1 - \frac{\alpha}{2}} + \mu^2 V^{1 + \frac{\alpha}{2}}) + \eta \tag{9}$$

where $\mu > 0$, $0 < \alpha < 1$, $T_c > 0$, $0 < \eta < \infty$.

Then the system (1) converges to a small domain \coprod close to the origin in a predefined time $\sqrt{2}T_c$. $\coprod = \left\{x \in {}^n \middle| V \leq \min\left\{\left(\frac{2\eta\alpha\mu T_c}{\pi}\right)^{\frac{2}{2-\alpha}}, \left(\frac{2\eta\alpha\mu^2 T_c}{\pi}\right)^{\frac{2}{2+\alpha}}\right\}\right\}.$

Proof 2: According to Eq. (9), one can obtain

$$\dot{V} \le -\frac{\pi}{\alpha\mu T_c} (\frac{1}{2} V^{1-\frac{\alpha}{2}} + \mu^2 V^{1+\frac{\alpha}{2}}) + (\eta - \frac{\pi}{\alpha\mu T_c} \frac{1}{2} V^{1-\frac{\alpha}{2}})$$
(10)

or

$$\dot{V} \le -\frac{\pi}{\alpha\mu T_c} (V^{1-\frac{\alpha}{2}} + \frac{1}{2}\mu^2 V^{1+\frac{\alpha}{2}}) + (\eta - \frac{\pi}{\alpha\mu T_c} \frac{\mu^2}{2} V^{1+\frac{\alpha}{2}})$$
(11)

For Eq. (10), when $V^{1-\frac{\alpha}{2}}>\frac{2\alpha\mu\eta T_c}{\pi}$, one can obtain $\dot{V}\leq-\frac{\pi}{\alpha\mu T_c}(\frac{1}{2}V^{1-\frac{\alpha}{2}}+\mu^2V^{1+\frac{\alpha}{2}})$. So the system (1) converges to this region $V^{1-\frac{\alpha}{2}}>\frac{2\alpha\mu\eta T_c}{\pi}$ in $\sqrt{2}T_c$.

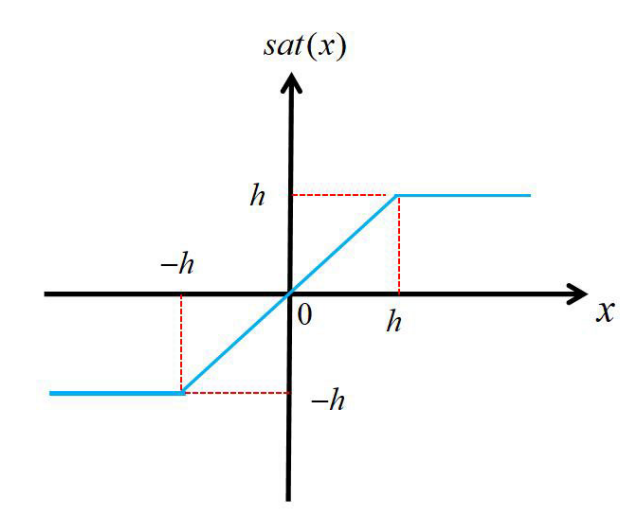


FIGURE 1. Saturation function.

For Eq. (11), when $V^{1+\frac{\alpha}{2}}>\frac{2\eta\alpha\mu T_c}{\pi\mu^2}$, one can obtain $\dot{V}\leq-\frac{\pi}{\alpha\mu T_c}(V^{1-\frac{\alpha}{2}}+\frac{1}{2}\mu^2V^{1+\frac{\alpha}{2}})$. So the system (1) converges to this region $V^{1+\frac{\alpha}{2}}>\frac{2\eta\alpha\mu T_c}{\pi\mu^2}$ in $\sqrt{2}T_c$. The detailed derivation of Proof 2 is similar to Lemma 2,

The detailed derivation of Proof 2 is similar to Lemma 2, so it is not presented here.

Lemma 4 [25]: If $x_1, x_2, \dots x_N$ are positive scalars and 0 < c < 1, d > 1, then one can obtain

$$\left(\sum_{i=1}^{N} |x_i|\right)^c \le \sum_{i=1}^{N} |x_i|^c$$

$$N^{1-d} \left(\sum_{i=1}^{N} |x_i|\right)^d \le \sum_{i=1}^{N} |x_i|^d$$
(12)

B. PROBLEM FORMULATION

Most systems such as robots and spacecraft are second-order nonlinear systems. Hence we take the following form as the model [26].

$$\dot{x}_1 = x_2
\dot{x}_2 = f_0(x) + g_0(x)u + E(x, t)$$
(13)

where $x = [x_1, x_2] \in \mathbb{R}^2$ denotes the states, $f_0(x)$ is a nonlinear function, $g_0(x)$ represents a known nonlinear smooth function, u specifies the controller input, E(x, t) denotes the external disturbance.

Assumption 1 [19]: The system uncertainties and disturbances are bounded: $|E(x, t)| \le D$, D > 0.

The goal of control is to design a control law *u* to make the system trajectory reach the desired trajectory.

The tracking error is

$$e_1 = x_1 - x_{1d}$$

$$e_2 = x_2 - \dot{x}_{1d}$$
(14)

where x_{1d} is the expected value of x_1 .

105572 VOLUME 11, 2023



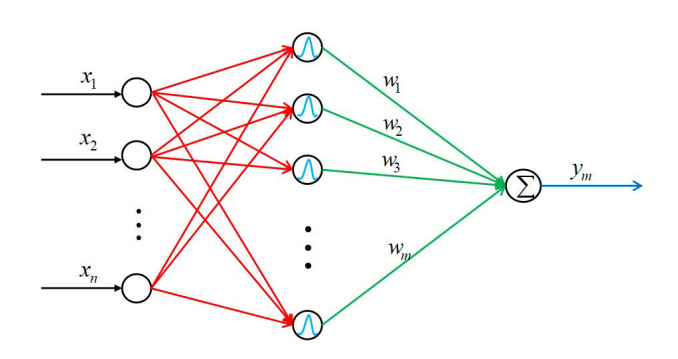


FIGURE 2. The structure of RBFNN.

Combining formula (13) and (14), one has

$$\dot{e}_1 = e_2
\dot{e}_2 = f_0(x) + g_0(x)u + E(x, t) - \ddot{x}_{1d}$$
(15)

III. A NEW PREDEFINED-TIME NONSINGULAR SMC

To ensure that e_1 converges in a predefined time during the sliding stage, we design a terminal sliding surface (TSS) as follows

$$s = \dot{e}_1 + b_1 |e_1|^{1-\alpha} sign(e_1) + b_2 |e_1|^{1+\alpha} sign(e_1)$$
 (16)

where
$$b_1=(\frac{1}{2})^{1-\alpha/2}\frac{\pi}{\alpha\mu_1T_1},\ b_2=(\frac{1}{2})^{1+\alpha/2}\frac{\mu_1\pi}{\alpha T_1},\ \mu_1>0,\ 0<\alpha<1,\ T_1>0.$$

Taking the derivative of Eq. (8), we can obtain

$$\dot{s} = \dot{e}_2 + b_1(1 - \alpha)|e_1|^{-\alpha}e_2 + b_2(1 + \alpha)|e_1|^{\alpha}e_2$$
 (17)

Substituting Eq.(15) into Eq.(17) to obtain the equivalent controller as

$$u_{eq} = -g_0^{-1}(x)[f_0(x) - \ddot{x}_{1d} + b_1(1-\alpha)|e_1|^{-\alpha}e_2 + b_2(1+\alpha)|e_1|^{\alpha}e_2]$$
 (18)

However, it can be seen that Eq. (18) contains a negative power term $|e_1|^{-\alpha}e_2$, which will lead to singularity when $e_1=0, e_2\neq 0$. In addition, it is difficult to obtain high-precision model information $f_0(x)$ in the actual control process.

Inspired by Reference [24], a SF is introduced into the controller to solve singular problems. The SF in the Figure 1 is defined as Eq. (19)

$$sat(x) = \begin{cases} x & x \le h \\ hsign(x) & x > h \end{cases}$$
 (19)

where h is a positive constant.

Then, the equivalent control law u_{eq} can be rewritten as

$$u_{eq1} = -g_0^{-1}(x)[f_0(x) - \ddot{x}_{1d} + sat[b_1(1-\alpha)|e_1|^{-\alpha}e_2] + b_2(1+\alpha)|e_1|^{\alpha}e_2]$$
(20)

The use of the SF limits the amplitude of the singular term $|e_1|^{-\alpha}e_2$.

Inspired by Reference [27], a RBFNN in Fig. 2 is employed to deal with $f_0(x)$.

The RBFNN algorithm is

$$h_j(x) = \exp(\frac{\|x - c_j\|^2}{2b_i^2})$$
 (21)

$$f_0(x) = W^{*T}h(x) + \varepsilon \tag{22}$$

where x is the input of the RBFNN, j is the jth node of the hidden layer of the RBFNN, $h(x) = [h_j(x)]^T$ is the output of the Gaussian basis function, W^* is the ideal weight of the RBFNN. And ε is the approximation error of the RBFNN, which satisfies $\varepsilon \le |\varepsilon|_{\max}$.

The model information is approximated by the RBFNN, which is in the form of

$$\hat{f}_0(x) = \hat{W}^T h(x) \tag{23}$$

$$\tilde{W} = \hat{W} - W^* \tag{24}$$

where $\hat{W} = [\hat{W}_1, \hat{W}_2, \dots, \hat{W}_m]$ is the actual weight value. \tilde{W} is the estimation error of the RBFNN weight.

Then, Eq. (20) can be rewritten as

$$u_{xeq} = -g_0^{-1}(x)[\hat{f}_0(x) - \ddot{x}_{1d} + b_1 e_2 + sat[b_2(1-\alpha)|e_1|^{-\alpha}e_2] + b_3(1+\alpha)|e_1|^{\alpha}e_2]$$
(25)

Therefore, the controller of the system is

$$u = u_{xeq} + u_{sw} \tag{26}$$

$$u_{sw} = -g_0^{-1}(x)[k_1|s|^{1-\beta}sign(s) + k_2|s|^{1+\beta}sign(s) + Ksign(s)]$$
(27)

where
$$k_1=(\frac{1}{2})^{1-\beta/2}\frac{\pi}{\beta\mu_2T_2},$$
, $k_2=(\frac{1}{2})^{1+\beta/2}\frac{\mu_2\pi}{\beta T_2},$ $\beta\in(0,1),$ $\mu_2>0,$ $T_2>0,$ $K>0.$

The block diagram of the proposed method can be found in Figure 3.

Remark 4: The existence of the Ksign(s) in the control law (27) may cause chattering. In order to reduce chattering, $\chi(\delta, s) = \frac{e^{\delta s} - 1}{e^{\delta s} + 1}$ is used to replace the sign function [28], $\delta > 0$.

IV. STABILITY ANALYSIS

For convenient of presentation, we define the following form

$$M = \{(e_1, e_2) : b_1(1 - \alpha)|e_1|^{-\alpha}e_2 \le h\}$$

$$N = \{(e_1, e_2) : b_1(1 - \alpha)|e_1|^{-\alpha}e_2 > h\}$$
(28)

Theorem 1: Assuming there is a positive constant K that satisfies $K > |E(x, t)| + |\varepsilon|_{\text{max}}$ and an adaptive law Eq. (25), the system (15) uses the controller (26), (25), (23), (27), the sliding variable will converge to a neighbor of zero in a predefined time $\sqrt{2}T_2$.

Proof 3: Taking into account

$$f_0(x) - \hat{f}_0(x) = W^{*T} h(x) + \varepsilon - \hat{W}^T h(x) = -\tilde{W}^T h(x) + \varepsilon$$
(29)

Construct the Lyapunov function by

$$V_1 = \frac{1}{2}s^2 + \frac{1}{2\gamma}\tilde{W}^T\tilde{W}$$
 (30)

where $\gamma > 0$.



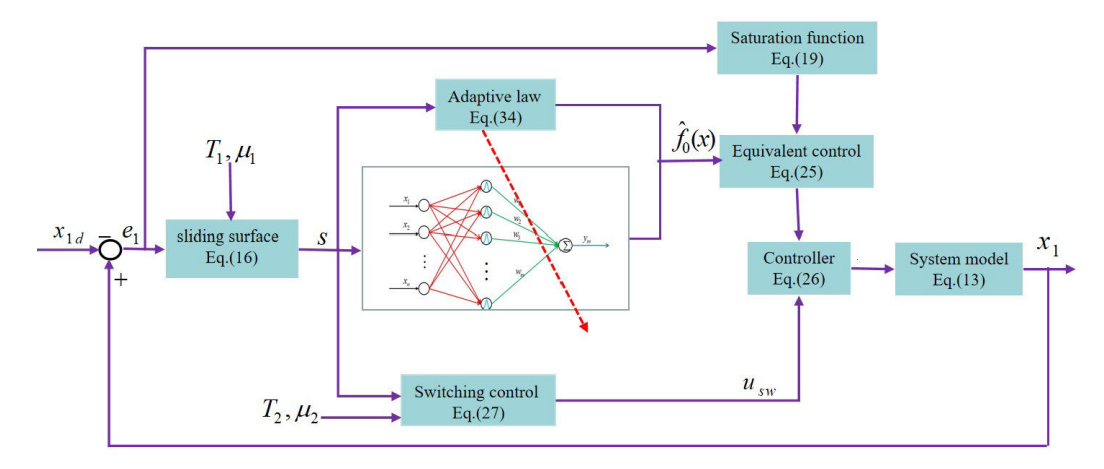


FIGURE 3. The block diagram of the predefined time nonsingular TSMC.

Taking derivative of Eq.(30), we have:

$$\begin{split} \dot{V}_{1} &= s \cdot \dot{s} + \frac{1}{\gamma} \tilde{W}^{T} \dot{\hat{W}} \\ &= s [\dot{e}_{2} + b_{1}(1 - \alpha)|e_{1}|^{-\alpha} e_{2} + b_{2}(1 + \alpha)|e_{1}|^{\alpha} e_{2}] \\ &+ \frac{1}{\gamma} \tilde{W}^{T} \dot{\hat{W}} \\ &= s [f_{0}(x) + g_{0}(x)u + E(x, t) - \ddot{x}_{1d} \\ &+ (b_{1}(1 - \alpha)|e_{1}|^{-\alpha} e_{2} + b_{2}(1 + \alpha)|e_{1}|^{\alpha} e_{2})] \\ &+ \frac{1}{\gamma} \tilde{W}^{T} \dot{\hat{W}} \end{split} \tag{31}$$

When (e_1, e_2) are in the area M, we can obtain

$$sat[b_1(1-\alpha)|e_1|^{-\alpha}e_2] = b_1(1-\alpha)|e_1|^{-\alpha}e_2$$
 (32)

Substituting Eq. (26) into Eq. (31), we can obtain

$$\dot{V}_{1} = s[f_{0}(x) - \hat{f}_{0}(x) - k_{1}|s|^{1-\beta}sign(s)
- k_{2}|s|^{1+\beta}sign(s) - Ksign(s) + E(x,t)]
= -k_{1}|s|^{2-\beta} - k_{2}|s|^{2+\beta} - |s|(K - E(x,t) - \varepsilon)
+ \tilde{W}^{T}[\frac{1}{\gamma}\dot{\hat{W}} - sh(x)]$$
(33)

The adaptive law is set to

$$\dot{\hat{W}} = \gamma s h(x) \tag{34}$$

Let $K > |E(x, t)| + |\varepsilon|_{\max}$, we can obtain

$$\dot{V}_{1} \leq -k_{1}|s|^{2-\beta} - k_{2}|s|^{2+\beta}
\leq -k_{1}|s^{2}|^{1-\frac{\beta}{2}} - k_{1}|\frac{1}{\gamma}\tilde{W}^{T}\tilde{W}|^{1-\frac{\beta}{2}}
- k_{2}|s^{2}|^{1+\frac{\beta}{2}} - k_{2}|\frac{1}{\gamma}\tilde{W}^{T}\tilde{W}|^{1+\frac{\beta}{2}}
+ k_{1}|\frac{1}{\gamma}\tilde{W}^{T}\tilde{W}|^{1-\frac{\beta}{2}} + k_{2}|\frac{1}{\gamma}\tilde{W}^{T}\tilde{W}|^{1+\frac{\beta}{2}}
\leq -k_{1}|s^{2}|^{1-\frac{\beta}{2}} - k_{1}|\frac{1}{\gamma}\tilde{W}^{T}\tilde{W}|^{1-\frac{\beta}{2}}
- k_{2}|s^{2}|^{1+\frac{\beta}{2}} - k_{2}|\frac{1}{\gamma}\tilde{W}^{T}\tilde{W}|^{1+\frac{\beta}{2}} + \Omega$$
(35)

where
$$\Omega = k_1 \left| \frac{1}{\gamma} \tilde{W}^T \tilde{W} \right|^{1 - \frac{\beta}{2}} + k_2 \left| \frac{1}{\gamma} \tilde{W}^T \tilde{W} \right|^{1 + \frac{\beta}{2}} > 0.$$
 From Lemma 4, it can be seen that

$$\dot{V}_1 \le -\frac{\pi}{\beta \mu_2 T_2} (V_1^{1-\frac{\beta}{2}} + \mu_2^2 V_1^{1+\frac{\beta}{2}}) + \Omega \tag{36}$$

According to Lemma 3, the sliding variable will converge to a neighbor of zero in a predefined time $\sqrt{2}T_2$.

Remark 5: The setting method of Ω is widely present in existing literature, for example, z_i in Reference [29] is a function related to the adaptive rates and is bounded. As is well known, the weight update rates of RBFNN are bounded. Ω is a function related to adaptive laws of the RBFNN, therefore it is bounded.

When (e_1, e_2) are in the area N, from Eq.(15), we can obtain

$$e_1(t) = e_1(0) + \int_0^t e_2(\tau)d\tau \tag{37}$$

When $e_2(t) > 0$, $e_1(t)$ will increase monotonically. When $e_2(t) < 0$, $e_1(t)$ will decrease monotonically. Described by Reference [24], (e_1, e_2) will leave the area M and not stay in that area forever. The existence of the area N doesn't impact the results of the stability analysis, the introduction of the SF doesn't degenerate the control performance, the time to travel through the area N is a very small proportion of the CT.

In summary, the sliding variable converges to a neighbor of zero in a predefined time $\sqrt{2}T_2$. This completes the proof.

Theorem 2: When the TSS s will converge to a neighbor of zero, the tracking error will converge to the origin in a predefined time T_1 .

Proof 4: The domain is arbitrarily small by designing appropriate parameters [29]. When the domain is approximately zero, $s(e_1) = 0$, we can obtain

$$\dot{e}_1 = -b_1|e_1|^{1-\alpha}sign(e_1) - b_2|e_1|^{1+\alpha}sign(e_1)$$
 (38)

Construct the Lyapunov function by

$$V_2 = \frac{1}{2}e_1^2 \tag{39}$$

105574 VOLUME 11, 2023



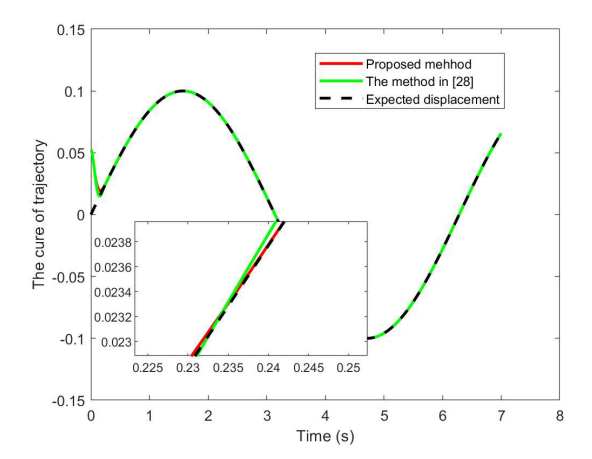


FIGURE 4. The cure of tracjectory.

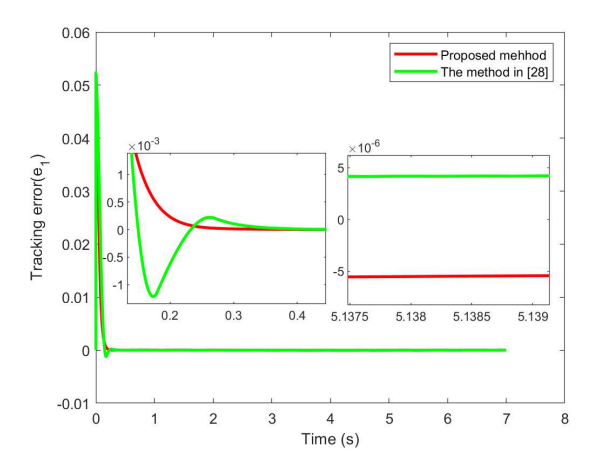


FIGURE 5. Tracking error.

The time derivative of the Eq.(39)

$$\dot{V}_{2} = e_{1}\dot{e}_{1}
= e_{1}[-b_{1}|e_{1}|^{1-\alpha}sign(e_{1}) - b_{2}|e_{1}|^{1+\alpha}sign(e_{1})]
= -b_{1}|e_{1}|^{2-\alpha} - b_{2}|e_{1}|^{2+\alpha}
= -\frac{\pi}{\alpha\mu_{1}T_{1}}(V_{2}^{1-\frac{\alpha}{2}} + \mu_{1}^{2}V_{2}^{1+\frac{\alpha}{2}})$$
(40)

According to Lemma 2, the tracking error converges within a predefined time T_1 . This ends the proof.

V. SIMULATION VERIFICATION

In order to verify the advantages of the proposed method, we select a inverted pendulum model for simulation verification, the dynamic system is as follows [27]

$$\ddot{\varphi} = \frac{g \sin \varphi - m_c l \dot{\varphi}^2 \cos \varphi \sin \varphi / (m + m_c)}{l[4/3 - m_c \cos^2 \varphi / (m + m_c)]} + \frac{[\cos \varphi / (m + m_c)]u}{l[4/3 - m_c \cos^2 \varphi / (m + m_c)]} + d(t)$$
(41)

where φ is angular displacement, u is control input. $d = \sin(10t) + \cos(t)$, m = 1kg, $m_c = 0.1kg$, l = 0.5m,

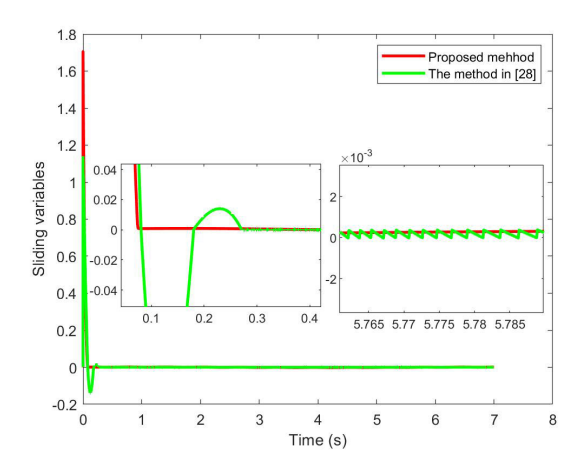


FIGURE 6. TSliding surface.

 $g=9.8m/s^2$. The initial value of the states are $\varphi(0)=\frac{\pi}{60}$, $\dot{\varphi}(0)=0$. Use appropriate control method to make $\varphi(t)$ move according to the desired trajectory $\varphi_d=0.1\sin(t)$. The Controller parameters are: $T_1=0.5, \, \mu_1=3, \, \alpha=0.4, \, h=0.5, \, T_2=1, \, \mu_2=3, \, \beta=0.4, \, \delta=400$.

Now we compare the proposed method with the nonsingular fixed time control. The compared control method has certain similarities with the proposed control method, such as items with an index greater than 1, items with an index less than 1, and the use of a SF.

The detailed expression for nonsingular fixed time control are as follows [28]

$$s = \dot{e}_{1} + c_{1}|e_{1}|^{\vartheta_{1}}sign(e_{1}) + c_{2}|e_{1}|^{\vartheta_{2}}sign(e_{1})$$
(42)

$$u = -g_{0}^{-1}(x)[f_{0}(x) - \ddot{x}_{1d} + sat(c_{1}\vartheta_{1}|e_{1}|^{\vartheta_{1}-1}\dot{e}_{1})$$

$$+ c_{2}\vartheta_{2}|e_{1}|^{\vartheta_{2}-1}\dot{e}_{1} + c_{3}|s|^{\vartheta_{3}}sign(s)$$

$$+ c_{4}|s|^{\vartheta_{4}}sign(s) + D_{2}sign(s)]$$
(43)

where c_1 , c_2 , c_3 , c_4 , $D_2 > 0$, $\vartheta_1 = \frac{m_1+1}{2} + \frac{1-m_1}{2} sign(|e_1|-1)$, $\vartheta_2 = \frac{m_2+1}{2} + \frac{m_2-1}{2} sign(|e_1|-1)$, $\vartheta_3 = \frac{n_1+1}{2} + \frac{1-n_1}{2} sign(|s|-1)$, $\vartheta_4 = \frac{n_2+1}{2} + \frac{n_2-1}{2} sign(|s|-1)$, $0 < m_1, n_1 < 1$, $m_2, n_2 > 1$

Figure 4 shows the curve of trajectory tracking, indicating that all controllers can achieve the expected goals, but the proposed method is the earliest to achieve the desired trajectory. Figure 5 shows the curve of tracking error, which indicates that the proposed control method has a short CT and small steady-state error.

Figure 6 shows the curve of the sliding surface, indicating that the proposed control method has the shortest convergence time and the best steady-state error. Figure 7 shows that the control output curve of the proposed method is the smoothest and meets the requirements of actual control engineering.

Figure 8 shows the convergence time of sliding variable and tracking error under different controllers. The actual convergence time is within the designed convergence time, and the designed convergence time does not depend on the

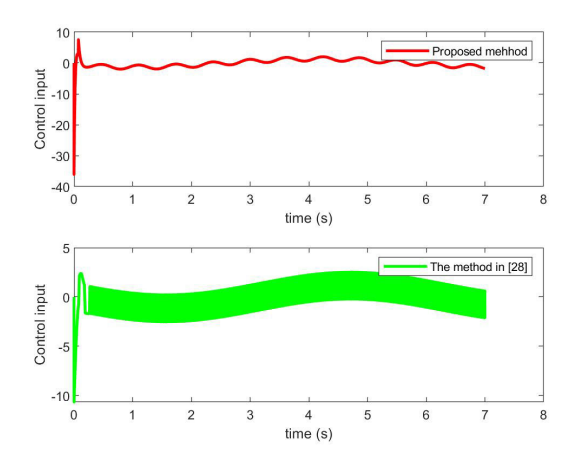


FIGURE 7. Control input.

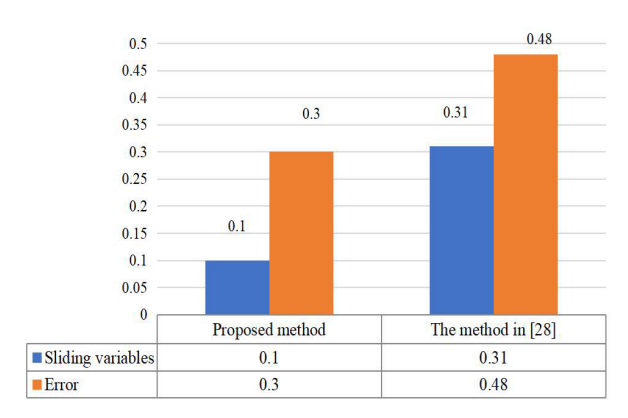


FIGURE 8. Convergence time.

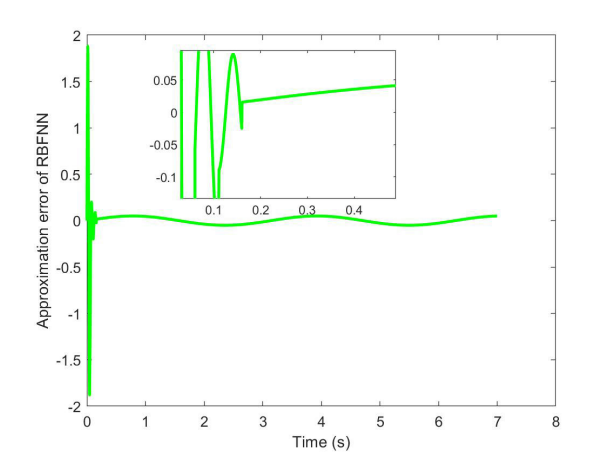


FIGURE 9. Approximate error of RBFNN.

parameters of the controller, which is more in line with the requirements of actual control engineering.

Figure 9 and 10 respectively show the approximation error and weight update law of RBFNN, indicating that RBFNN has a good ability to approximate nonlinear functions, and the approximation error is within the allowable range.

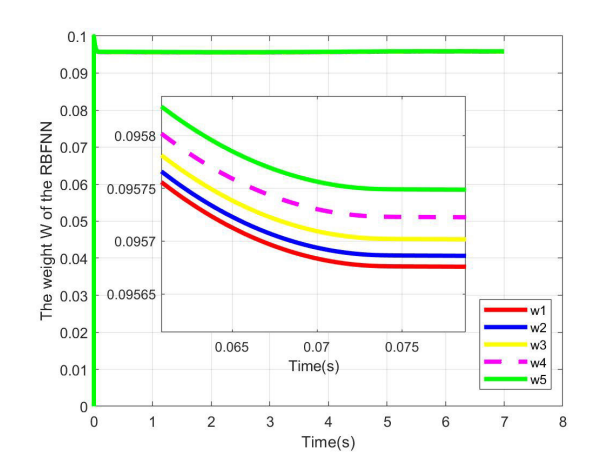


FIGURE 10. The weight W of RBFNN.

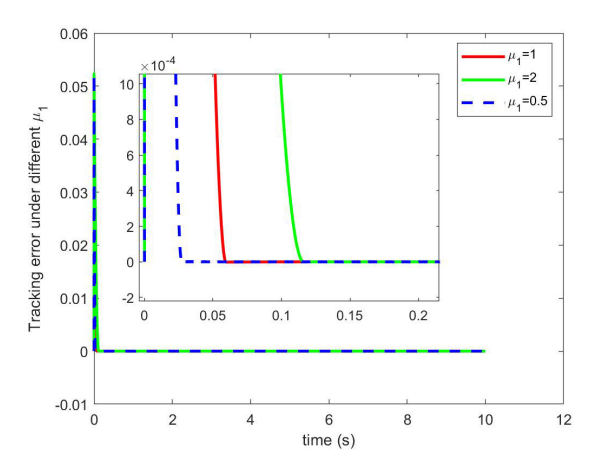


FIGURE 11. Tracking error under different μ_1 .

Figure 11 shows that by adjusting a parameter μ_1 , the actual CT of the tracking error can be changed. When $\mu_1 = 2$, the CT is longer than $\mu_1 = 1$. When $\mu_1 = 0.5$, the CT is shorter than $\mu_1 = 1$.

VI. CONCLUSION

This paper proposes a novel predefined time nonsingular TSMC based on RBFNN, which ensures that the tracking error can be predefined time stable in both the arrival and sliding stages. RBFNN is used to approximate nonlinear functions to solve the problem of unknown system model information. And the singular problem of TSMC was solved by using a SF. Finally, the proposed method has been verified to have good control performance through comparative simulation. However, faults will occur in actual control engineering, and fault-tolerant control will be further analyzed in future work.

REFERENCES

- J. Chao and W. Aiguo, "A new control method for multi cylinder hydraulic press," *J. Huazhong Univ. Sci. Technol. Natural Sci. Ed.*, vol. 41, no. 9, pp. 42–47, 2013.
- [2] M. Van and D. Ceglarek, "Robust fault tolerant control of robot manipulators with global fixed-time convergence," *J. Franklin Inst.*, vol. 358, no. 1, pp. 699–722, Jan. 2021.

105576 VOLUME 11, 2023



- [3] H. Ye, M.-M. Li, W.-G. Luo, and Y.-X. Qin, "Finite-time consensus of heterogeneous multi-agent systems without velocity measurements and with disturbances via integral sliding mode control," *IEEE Access*, vol. 6, pp. 62255–62260, 2018.
- [4] J. Ren, S. Tang, and T. Chen, "Adaptive sliding mode control of spacecraft attitude-orbit dynamics on SE(3)," Adv. Space Res., vol. 71, no. 1, pp. 525–538, Jan. 2023.
- [5] L. Yipeng, C. Qilin, H. Xuecheng, and L. Y ufei, "Research on nonfragile robust control of magnetic levitation permanent magnet linear motor control system," *J. Electr. Eng. Technol.*, vol. 31, no. 7, pp. 42–47, 2016.
- [6] C. Ziyin, L. Zhe, K. Jianbing, J. Heming, and Y. Fei, "Servo control of threephase permanent magnet synchronous motor based on command filtered backstepping," *Control Theory Appl.*, vol. 34, no. 4, pp. 142–147, 2017.
- [7] H. O. Ozer, Y. Hacioglu, and N. Yagiz, "High order sliding mode control with estimation for vehicle active suspensions," *Trans. Inst. Meas. Control*, vol. 40, no. 5, pp. 1457–1470, Mar. 2018.
- [8] Y. Feng, F. Han, and X. Yu, "Chattering free full-order sliding-mode control," *Automatica*, vol. 50, no. 4, pp. 1310–1314, Apr. 2014.
- [9] J. Yu, P. Shi, and L. Zhao, "Finite-time command filtered backstepping control for a class of nonlinear systems," *Automatica*, vol. 92, pp. 173–180, Jun. 2018.
- [10] M. Labbadi and M. Cherkaoui, "Robust adaptive backstepping fast terminal sliding mode controller for uncertain quadrotor UAV," *Aerosp. Sci. Technol.*, vol. 93, Oct. 2019, Art. no. 105306.
- [11] F. Assegaf, R. Saragih, and D. Handayani, "Adaptive sliding mode control for cholera epidemic model," *IFAC-PapersOnLine*, vol. 53, no. 2, pp. 16092–16099, 2020.
- [12] S. P. Bhat and D. S. Bernstein, "Finite-time stability of continuous autonomous systems," SIAM J. Control Optim., vol. 38, no. 3, pp. 751–766, Jan. 2000.
- [13] X. Yu and M. Zhihong, "Fast terminal sliding-mode control design for nonlinear dynamical systems," *IEEE Trans. Circuits Syst. I, Fundam. Theory Appl.*, vol. 49, no. 2, pp. 261–264, 2002.
- [14] A. Polyakov, "Nonlinear feedback design for fixed-time stabilization of linear control systems," *IEEE Trans. Autom. Control*, vol. 57, no. 8, pp. 2106–2110, Aug. 2012.
- [15] W. Jinxiu, Z. Huijie, and S. Yuyao, "A distributed predefined-time attitude coordination control scheme for multiple rigid spacecraft," *Aerosp. Sci. Technol.*, vol. 133, Feb. 2023, Art. no. 108134.
- [16] M. Chaoyong, L. Inseok, H. Feng, and W. Yue, "Attitude control of rigid spacecraft with predefined-time stability," *J. Franklin Inst.*, vol. 357, no. 7, pp. 4212–4221, May 2020.
- [17] G. Yu, Z. Li, H. Liu, and Q. Zhu, "Predefined time nonsingular fast terminal sliding mode control for trajectory tracking of ROVs," *IEEE Access*, vol. 10, pp. 107864–107876, 2022.
- [18] E. Jiménez-Rodríguez, A. J. Muñoz-Vázquez, J. D. Sánchez-Torres, M. Defoort, and A. G. Loukianov, "A Lyapunov-like characterization of predefined-time stability," *IEEE Trans. Autom. Control*, vol. 65, no. 11, pp. 4922–4927, Nov. 2020.
- [19] F. Wang, Y. Miao, C. Li, and I. Hwang, "Attitude control of rigid spacecraft with predefined-time stability," *J. Franklin Inst.*, vol. 357, no. 7, pp. 4212–4221, May 2020.
- [20] C. Wu, J. Yan, J. Shen, X. Wu, and B. Xiao, "Predefined-time attitude stabilization of receiver aircraft in aerial refueling," *IEEE Trans. Circuits* Syst. II, Exp. Briefs, vol. 68, no. 10, pp. 3321–3325, Oct. 2021.
- [21] Z. Ruan, Y. Li, J. Hu, J. Mei, and D. Xia, "Finite-time synchronization of the drive-response networks by event-triggered aperiodic intermittent control," *Neurocomputing*, vol. 485, pp. 89–102, May 2022.

- [22] H. Chen, G. Tang, Y. Huang, J. Wang, and H. Huang, "Adaptive model-parameter-free nonsingular fixed-time sliding mode control for underwater cleaning vehicle," *Ocean Eng.*, vol. 262, Oct. 2022, Art. no. 112239.
- [23] H. Zhou, Y. Zhang, W. Duan, and H. Zhao, "Nonlinear systems modelling based on self-organizing fuzzy neural network with hierarchical pruning scheme," *Appl. Soft Comput.*, vol. 95, Oct. 2020, Art. no. 106516.
- [24] Y. Feng, X. Yu, and F. Han, "On nonsingular terminal sliding-mode control of nonlinear systems," *Automatica*, vol. 49, no. 6, pp. 1715–1722, Jun. 2013.
- [25] L. Cui, N. Jin, S. Chang, Z. Zuo, and Z. Zhao, "Fixed-time ESO based fixed-time integral terminal sliding mode controller design for a missile," *ISA Trans.*, vol. 125, pp. 237–251, Jun. 2022.
- [26] C. Jia, D. Kong, and L. Du, "Recursive terminal sliding-mode control method for nonlinear system based on double hidden layer fuzzy emotional recurrent neural network," *IEEE Access*, vol. 10, pp. 118012–118023, 2022.
- [27] X. Sun, L. Zhang, and J. Gu, "Neural-network based adaptive sliding mode control for Takagi–Sugeno fuzzy systems," *Inf. Sci.*, vol. 628, pp. 240–253, May 2023.
- [28] Y. Tian, Y. Cai, and Y. Deng, "A fast nonsingular terminal sliding mode control method for nonlinear systems with fixed-time stability guarantees," *IEEE Access*, vol. 8, pp. 60444–60454, 2020.
- [29] Z. Gao, Y. Zhang, and G. Guo, "Fixed-time prescribed performance adaptive fixed-time sliding mode control for vehicular platoons with actuator saturation," *IEEE Trans. Intell. Transp. Syst.*, vol. 23, no. 12, pp. 24176–24189, Dec. 2022.



CHAO JIA received the B.E. and M.E. degrees from the Tianjin University of Technology, Tianjin, China, in 2002 and 2008, respectively, and the Ph.D. degree from Tianjin University, Tianjin, in 2013. He joined the School of Electrical Engineering and Automation, Tianjin University of Technology, in 2002, becoming an Associate Professor, in 2013. He was a Visiting Scholar with Columbia University, NY, USA, from 2016 to 2017. From 2023, he is also a Visiting

Scholar with Tsinghua University, Beijing, China. His current research interests include nonlinear control, adaptive control, and intelligent control and their application.



XIAOHUA LIU received the B.S. degree in electrical engineering and automation from the Qilu University of Technology, Shandong, in 2021. He is currently pursuing the M.S. degree with Tianjin University of Technology, Tianjin, China. His research interests include nonlinear control, adaptive higher-order sliding mode control, intelligent control, predefined time control, barrier function, and nonsingular control.

• • •